Supplementary Information for "Identifying pragmatic quasi-harmonic electronic structure approaches for modeling molecular crystal thermal expansion"

Jessica L. McKinley and Gregory J. O. Beran*

Department of Chemistry, University of California, Riverside, California 92521 USA

E-mail: gregory.beran@ucr.edu

February 25, 2018

Contents

*To whom correspondence should be addressed

S1 Construction of crystalline Gibbs free energies

The crystalline Gibbs free energies at various temperatures are constructed by combining the temperature-independent electronic energy curves (e.g. Figure S1a,d) with the Helmholtz vibrational free energy F_{vib} (e.g. Figure S1b,e) to give the free energy curves shown in Figure S1c,f. The optimal volume occurs at the minimum of the free energy curve. For carbon dioxide, the Tier 1–3 energy-volume curves are nearly identical, but the differences in the phonons lead to modest shifts in the position of the minima. At 0 K, Tiers 1–3 still exhibit almost the same minimum, but by 190 K, the optimal volumes differ somewhat.

Analogous plots are shown for ice at 0 K and 200 K in Figure S2. Ice has the unusual behavior that Tier 3 exhibits volume contraction upon adding the zero-point vibrational contribution. The reasons for this behavior can be seen in the plots. The optimal volume for the electronic energy curves of ice varies, with Tier 4 $<$ Tier 1/2 $<$ Tier 3. The MP2 Helmholtz vibrational free energy contribution decreases monotonically with volume, while the F_{vib} derived from B86bPBE-XDM phonons using either MP2 or DFT geometries is quite flat and exhibits a shallow minimum. In the Tier 2 and Tier 4 cases, the minimum of F_{vib} occurs at a volume greater than the $E(V)$ minimum, so adding F_{vib} to $E(V)$ to form the Gibbs free energy shifts the system toward larger volumes. In Tier 3, on the other hand, the minimum in $E(V)$ occurs at a larger volume than that of the B86bPBE-XDM F_{vib}, so the zero-point vibrational energy contribution shifts it toward smaller volumes, as seen in Figure 2 in the main paper. The large difference in slopes of F_{vib} largely accounts for the differences in thermal expansion between Tier 1 and the other Tiers. As the crystal is heated, the minimum in F_{vib} shifts toward larger volumes (e.g. see 200 K plots). Therefore, thermal expansion occurs as usual at higher temperatures.

Figures S3 and S4 present similar plots for acetic acid and imidazole. For acetic acid, the energy-volume and Helmholtz vibrational free energies are quite similar across the different tiers. For imidazole, the DFT results differ appreciably from MP2 due to the problems MP2 has describing the van der Waals dispersion in that crystal.

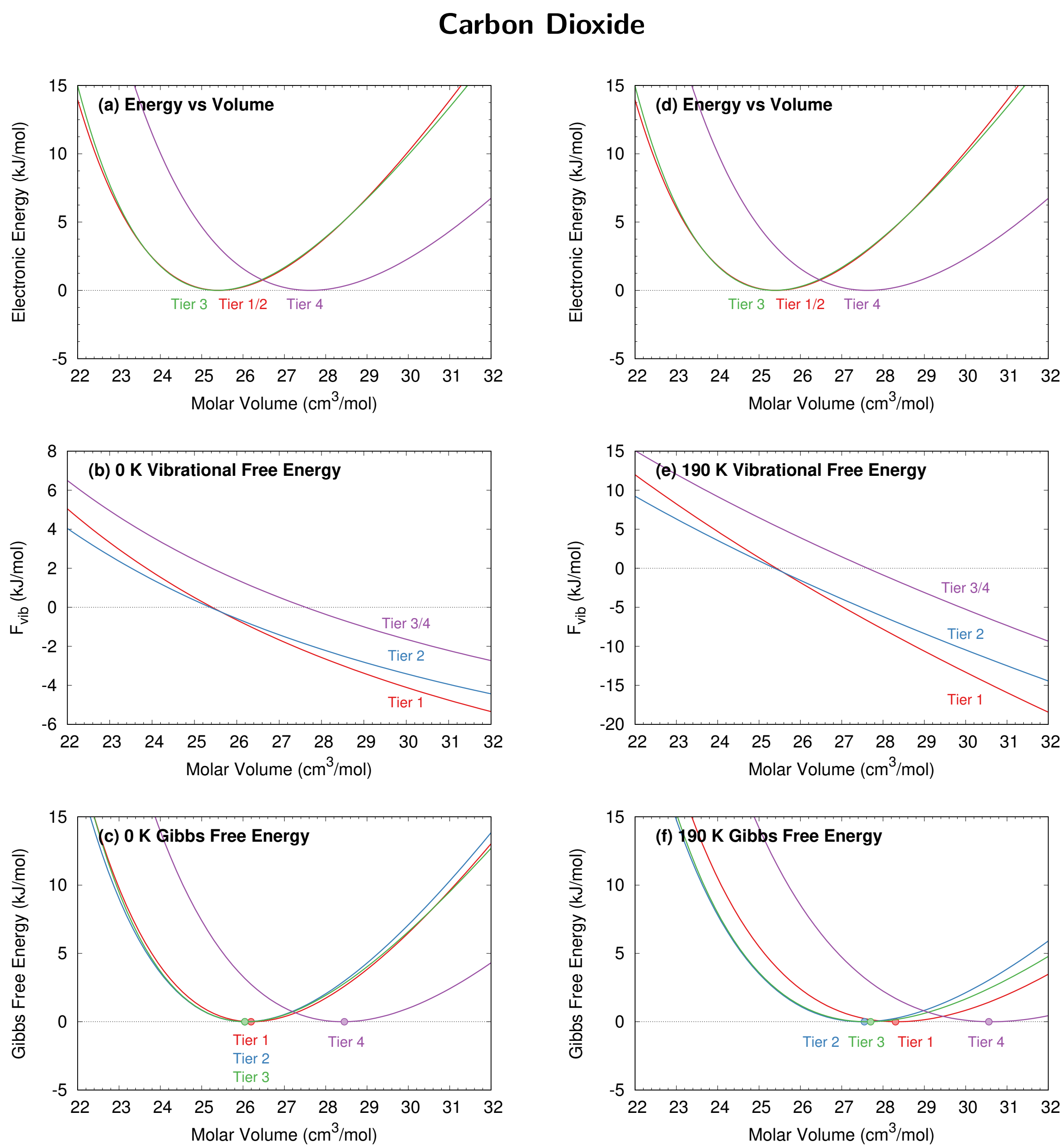

Figure S1: (a) Electronic energy versus volume curves, (b) 0 K vibrational free energies, and (c) total Gibbs free energies per unit cell with different mixtures of MP2/aug-cc-pVTZ + AMOEBA and B86bPBE-XDM. Plots (d)–(f) are the same but at 190 K. Energies correspond to the full unit cell, and arbitrary vertical offsets were employed to each curve for ease of viewing. Points indicate minima.

Ice

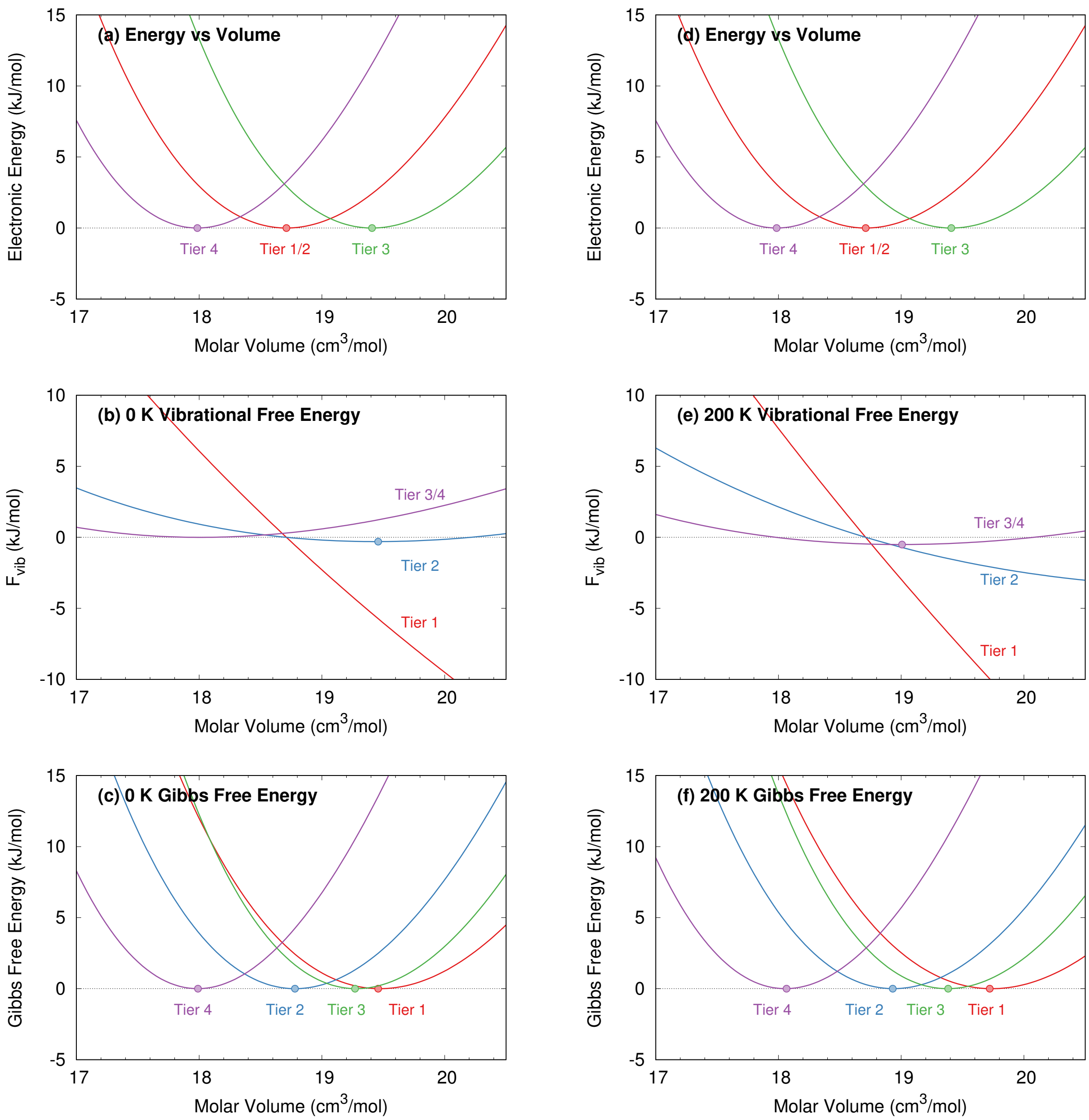

Figure S2: (a) Electronic energy versus volume curves, (b) 0 K vibrational free energies, and (c) total Gibbs free energies per unit cell with different mixtures of MP2/aug-cc-pVTZ + AMOEBA and B86bPBE-XDM. Plots (d)–(f) are the same but at 200 K. Energies correspond to the full unit cell, and arbitrary vertical offsets were employed to each curve for ease of viewing. Points indicate minima.

Acetic Acid

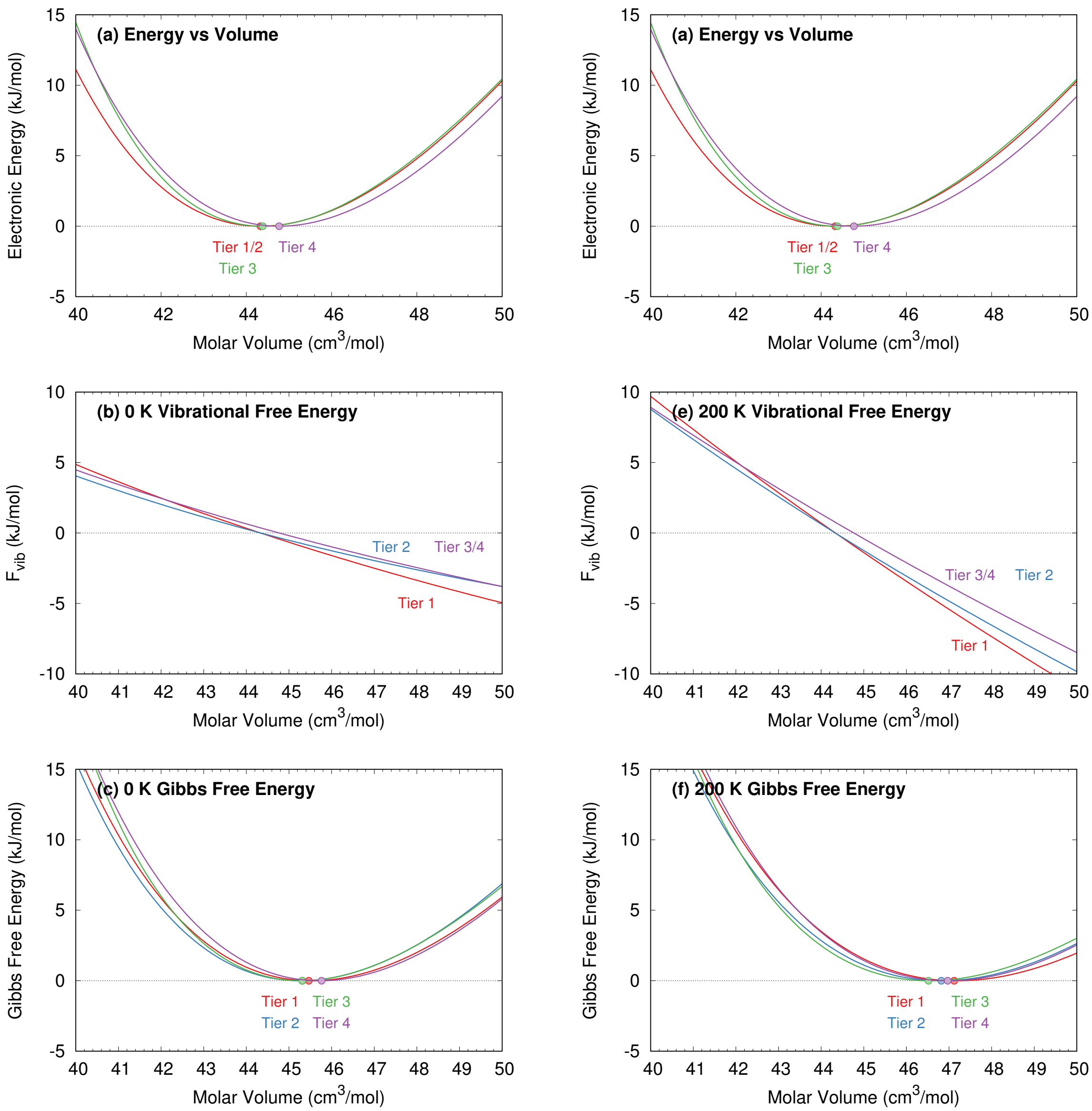

Figure S3: (a) Electronic energy versus volume curves, (b) 0 K vibrational free energies, and (c) total Gibbs free energies per unit cell with different mixtures of MP2/aug-cc-pVTZ + AMOEBA and B86bPBE-XDM. Plots (d)–(f) are the same but at 200 K. Energies correspond to the full unit cell, and arbitrary vertical offsets were employed to each curve for ease of viewing. Points indicate minima.

Imidazole

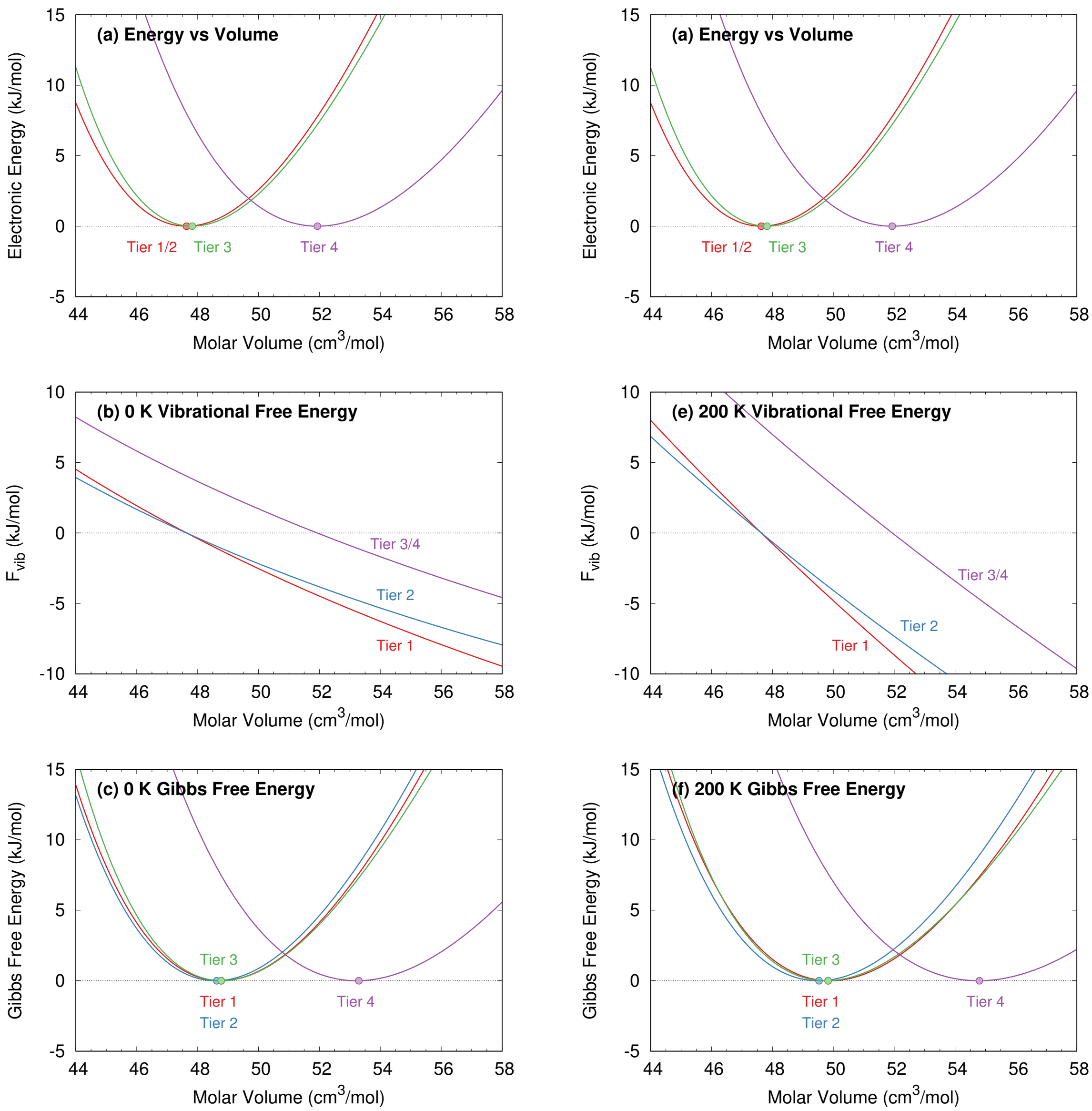

Figure S4: (a) Electronic energy versus volume curves, (b) 0 K vibrational free energies, and (c) total Gibbs free energies per unit cell with different mixtures of MP2/aug-cc-pVTZ + AMOEBA and B86bPBE-XDM. Plots (d)–(f) are the same but at 200 K. Energies correspond to the full unit cell, and arbitrary vertical offsets were employed to each curve for ease of viewing. Points indicate minima.

S2 Negative thermal expansion in ice Ih

Figure S5 focuses on the temperature dependence of the molar volume of ice in the low-temperature region, highlighting the negative thermal expansion. For ease of comparison, the volumes are plotted relative to the lowest-temperature volume for each case. Experimentally, ice contracts by 0.01 cm^3/mol (0.06%) upon heating to around 70 K. As shown here, all the models do predict some contraction, though it is barely noticeable for Tier 2. On the other hand, Tier 3 and Tier 4 predict the temperature of maximum contraction fairly well, though they underestimate the amount of contraction by a factor of 2–3.

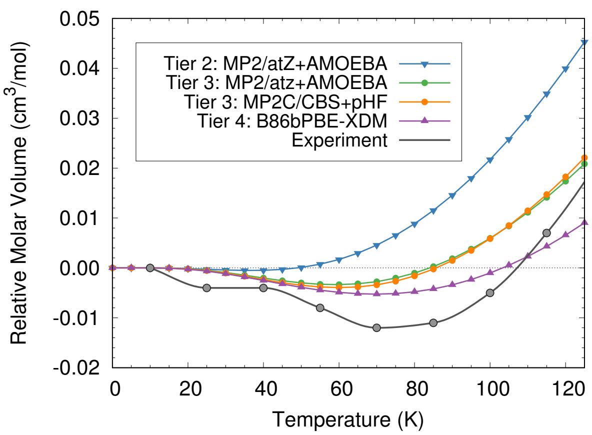

Figure S5: Comparison of predicted and experimental molar volumes for ice showing the degree to which various models predict the negative thermal expansion at low temperatures.

Table S1: Comparison of experimental and predicted % contraction of the unit cell from 10 K - 70 K

Method	Source	% Contraction
Experiment	Ref 1	0.06
B86bPBE-XDM	Tier 4	0.029
MP2/aTZ+AMOEBA	Tier 3	0.017
MP2/CBS+pHF	Tier 3	0.023
MP2C/CBS+pHF	Tier 3	0.021
MP2/aTZ+AMOEBA	Tier 2	0.003
MP2/aTZ+AMOEBA	Tier 1	0.010

S3 Sensitivity to choice of density functional

To complement the carbon dioxide results shown in Figure 4 of the main paper, Figure S6 compares the energy-volume curves and Helmholtz vibrational free energies of crystalline carbon dioxide at 150 K across several different density functionals. While the DFT $E(V)$ curves vary considerably with the choice of functional, the F_{vib} curves exhibit generally similar slopes. This helps explain why the Tier 2 and 3 molar volumes less sensitive to the choice of density functional used to generate the phonons.

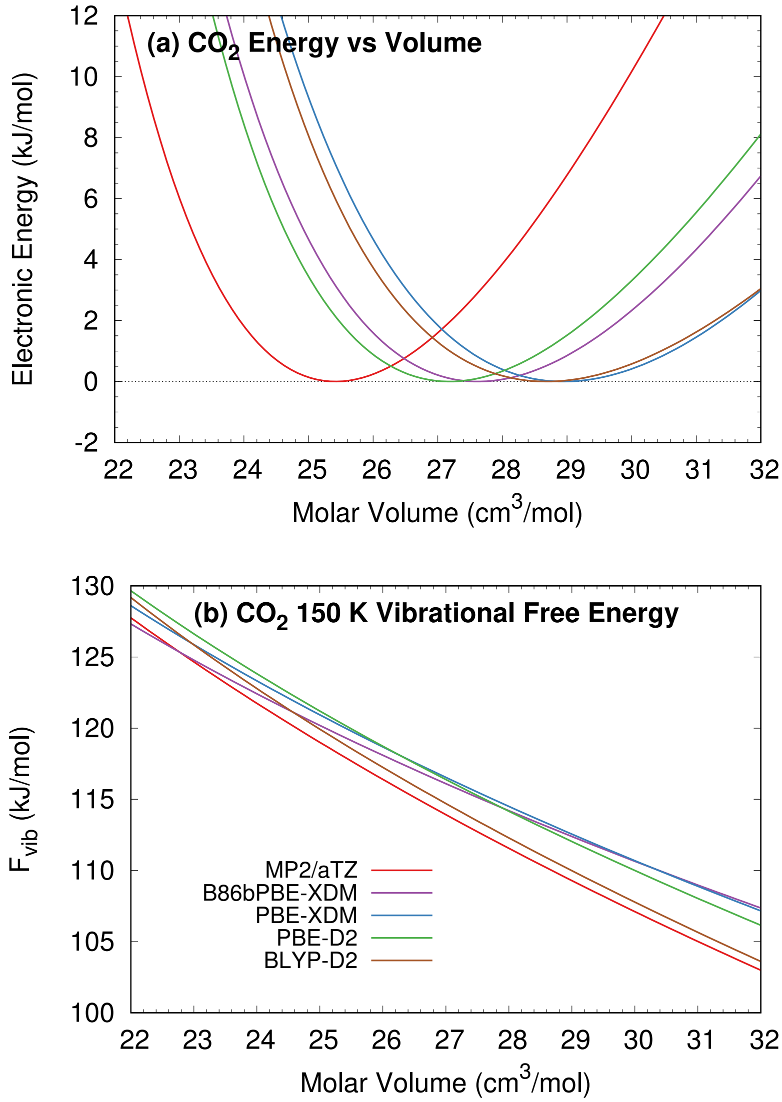

Figure S6: Variations in (a) the energy-volume curves and (b) 150 K Helmholtz vibrational free energies of carbon dioxide with several different density functionals. For ease of comparison, the energy-volume curves in (a) were shifted relative to their individual minimum energies.

To complement the carbon dioxide data presented in Figure 4 of the main paper, Figure S7 plots how ice molar volumes predicted with Tiers 2-4 vary with the choice of density functional. As for carbon dioxide, Tiers 2 and 3 are much less sensitive to the specific density functional used than Tier 4.

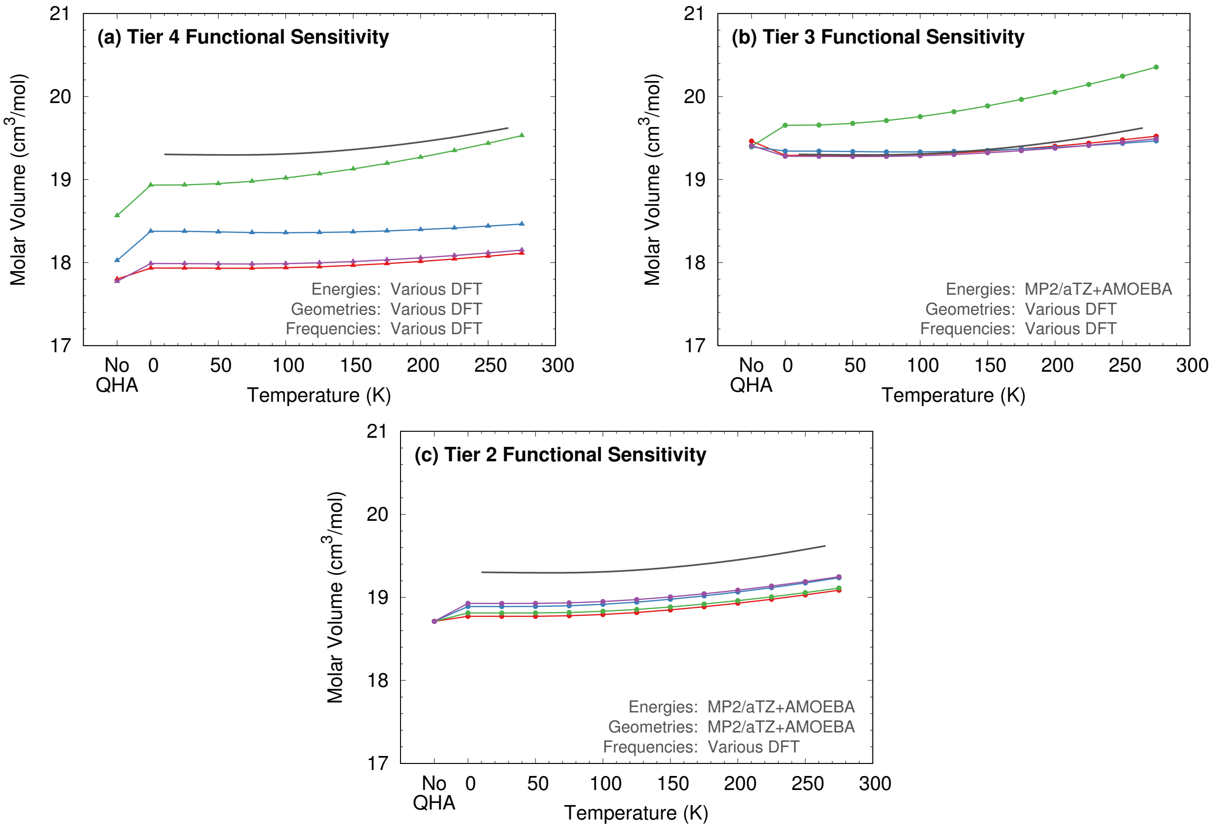

Figure S7: Sensitivity of the predicted ice molar volume to the density functional used for the low level in Tiers 2–4. Density functionals: PBE-XDM (red), BLYP-XDM (blue), BLYP-D2 (green), and B86bPBE-XDM (purple).

S4 Tier 3 energy refinement

As discussed in the main paper, different Tier 3 single-point energy refinements lead to molar volume curves that are largely parallel. This indicates that while the refinement does shift the energy and volume at which the minimum occurs, it does not significantly alter the well curvature.

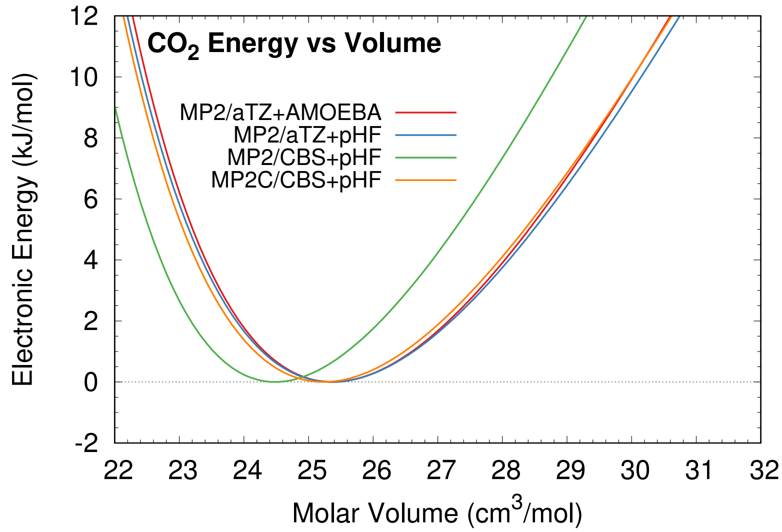

Figure S8: The Tier 3 single-point energy refinements for carbon dioxide do not significantly alter the curvature of the electronic energy well. For ease of comparison, the volumes are plotted relative to the lowest-temperature volume for each case.

References

(1) Petrenko, V. F.; Whitworth, R. W. *Physics of Ice*; Oxford University Press, 1999.